

## In Vivo Optical Imaging of Folate Receptor- $\beta$ in Head and Neck Squamous Cell Carcinoma

Joel Y. Sun, BA; Jiayin Shen, PhD; Joel Thibodeaux, MD; Gang Huang, PhD; Yiguang Wang, PhD;  
Jinming Gao, PhD; Philip S. Low, PhD; Dimiter S. Dimitrov, PhD; Baran D. Sumer, MD

**Objectives/Hypothesis:** Folate receptor (FR) expression, although known to be elevated in many types of cancer and inflammatory cells, has not been well characterized in head and neck squamous cell carcinoma (HNSCC). We hypothesized that tumor infiltrating inflammatory cells expressing FR- $\beta$  could allow fluorescent visualization of HNSCC tumors using folate conjugated dyes even when FR expression in cancer cells is low.

**Study Design:** Retrospective review of clinical pathologic specimens and in vivo animal study.

**Methods:** A tissue microarray with tumor and tumor-free tissue from 22 patients with HNSCC was stained with antibodies to FR- $\alpha$  and FR- $\beta$ . We characterized FR- $\beta^+$  cells by examining CD45, CD68, CD206, and transforming growth factor (TGF)- $\beta$  expression. To investigate fluorescent imaging, mice with orthotopic tumor xenografts were imaged in vivo after intravenous injections of folate conjugated fluorescein isothiocyanate (folate-FITC) and were histologically evaluated ex vivo.

**Results:** All tumor samples demonstrated significant FR- $\beta$  staining and negligible FR- $\alpha$  staining. FR- $\beta^+$  cells found in tumors coexpressed CD68 and had increased expression of CD206 and TGF- $\beta$  characteristic of tumor-associated macrophages. In the xenograft models, tumors showed strong in vivo fluorescence after folate-FITC injection in contrast to surrounding normal tissues. Histologic examination of the xenograft tissue similarly showed folate-FITC uptake in areas of inflammatory cellular infiltrate.

**Conclusions:** Although HNSCC tumor cells do not express FR, HNSCC tumors contain a significant population of FR- $\beta$ -expressing macrophages. Folate conjugated fluorescent dye is able to specifically target and label tumor xenografts to permit macroscopic fluorescence imaging due to FR- $\beta$  expression on the infiltrating inflammatory cells.

**Key Words:** Head and neck, squamous cell carcinoma, folate receptor, optical imaging, fluorescence, tumor-associated macrophages.

**Level of Evidence:** NA

*Laryngoscope*, 124:E312-E319, 2014

### INTRODUCTION

In the United States, head and neck cancer, represented mainly by head and neck squamous cell carcinoma (HNSCC), has an annual incidence of over 52,000 new cases and causes over 11,000 annual deaths.<sup>1</sup> Despite several decades of advancements in treatment, the mortality

of HNSCC remains high, and the recurrence rate for locally advanced disease can reach 50%.<sup>2</sup> The surgical resection of head and neck cancers requires high precision to maximize tumor removal without compromising the many complex functions carried out in the upper aerodigestive tract and neck. Techniques to improve the real-time intraoperative visualization of tumors are needed to increase the efficacy and decrease the morbidity of HNSCC resection. One strategy to improve the visualization of malignant tissues is the use of tumor-specific ligand conjugated fluorescent dyes.<sup>3-5</sup> Surgery guided by probes that optically highlight tumors can lead to better surgical margins and improve survival.<sup>6-8</sup> Many methods for the delivery of fluorescent probes into tumors have been explored.<sup>4,6,9,10</sup> Of these, folic acid conjugated fluorescent dyes that target the aberrant expression of folate receptors is one of the most mature platforms for use in fluorescence-guided tumor resection.

The folate receptor (FR) is a high-affinity folic acid binding endocytic receptor uncommonly expressed in normal tissues. The  $\alpha$  isoform (FR- $\alpha$ ) is normally found on the apical surface of polarized epithelial cells in tissues such as the proximal kidney tubule and the submandibular salivary gland.<sup>11</sup> Furthermore, it is overexpressed at high frequencies in a variety of carcinomas including those of the ovaries, kidneys, and lung.<sup>11-14</sup>

From the Department of Otolaryngology (J.Y.S., B.D.S.), Department of Pathology (J.T.), and Department of Pharmacology (G.H., Y.W., J.G.), University of Texas Southwestern Medical Center, Dallas, Texas; Department of Chemistry (J.S., P.S.L.), Purdue University, West Lafayette, Indiana; National Cancer Institute (D.S.D.), National Institutes of Health, Frederick, Maryland, U.S.A.

Editor's Note: This Manuscript was accepted for publication January 13, 2014.

A portion of the study was presented at the American Head and Neck Society Meeting at COSM, Orlando, Florida, U.S.A., April 11, 2013.

This study was supported by the Cancer Prevention and Research Institute of Texas grant RP120094 to B.D.S. and J.G.

Philip Low, PhD, holds the position of Chief Science Officer of Endocyte, Inc.

The authors have no other funding, financial relationships, or conflicts of interest to disclose.

Send correspondence to Baran D. Sumer, MD, UT Southwestern Medical Center, Simmons Comprehensive Cancer Center, Department of Otolaryngology-Head and Neck Surgery, 5323 Harry Hines Boulevard, Dallas, TX 75390. E-mail: baran.sumer@UTSouthwestern.edu

DOI: 10.1002/lary.24606

In contrast, functional expression of the  $\beta$  isoform (FR- $\beta$ ) is limited to a specific subset of activated macrophages and myeloid leukemia.<sup>11,15</sup> Importantly, the binding and expression characteristics of FR make it an ideal target for the intracellular delivery of tumor specific drugs and imaging markers. Clinical trials are underway for several folate-linked molecules including folate-fluorescein isothiocyanate (folate-FITC), which has been used for tumor-specific fluorescence-guided surgery in patients with ovarian cancer.<sup>9</sup>

However, the utility of the FR as a biomarker in HNSCC molecular imaging is unclear due to an incomplete characterization of the receptor's expression. Previous mRNA expression and radioligand binding assays on a limited number of tumor specimens have found FR- $\alpha$  expression to be negligible in HNSCC.<sup>12,16</sup> In contrast, immunohistochemistry performed on specimens from a larger patient sample detected FR expression of an unknown isoform in 45% of primary HNSCC tumors and 40% of lymph node metastases.<sup>17</sup> Furthermore, FR expression in the aforementioned study was inversely correlated with disease-free survival after surgery.<sup>17</sup> A more thorough examination of FR expression in HNSCC is required to assess the clinical potential of folate conjugated agents in the management of head and neck cancer. In this study, we characterize the expression pattern of the two main isoforms of folate receptor, FR- $\alpha$  and FR- $\beta$ , in HNSCC patient specimens. We then report on the use of folate-FITC to specifically target and optically image HNSCC in mouse tumor xenograft models.

## MATERIALS AND METHODS

### Tissue Samples

Human primary tumor samples were obtained from patients undergoing primary surgery for squamous cell carcinoma of the head and neck between 2007 and 2011. Patients who had previously undergone treatment for head and neck cancer were excluded. Tumor samples and adjacent tumor-free surgical margins were taken from 25 patients with HNSCC. Primary tumor sites included the oral tongue, base of tongue, tonsil, supraglottic larynx, glottic larynx, and hypopharynx. The clinical characteristics of the specimens used for the tissue microarray are shown in Table I. Tissue samples were obtained with approval from the institutional review board of the University of Texas Southwestern Medical Center in Dallas, Texas.

### Tissue Microarray Construction and Immunohistochemistry

A tissue microarray (TMA) was constructed by paraffin embedding 44 flash frozen samples from 22 patients. All samples were processed with the approval and under the guidelines of the University of Texas Southwestern institutional review board. Immunohistochemical staining was performed to evaluate the expression of FR- $\alpha$ , FR- $\beta$ , and CD68 on 4- $\mu$ m TMA sections. FR- $\alpha$  was detected using the monoclonal antibody (mAb) 343. TMA scoring of FR- $\alpha$  expression was done using stains from this antibody. FR- $\alpha$  staining was later replicated using mAb 26B3 and corresponding immunoglobulin G (IgG) isotype control (Biocare Medical, Concord, CA).<sup>18</sup> FR- $\beta$  was stained using biotinylated m909.<sup>19</sup> CD68 was stained using mAb PG-M1 (Dako, Carpinteria, CA). A general immunohistochemical

TABLE I.  
Clinical Characteristics of Specimens Used for the Construction of the Tissue Microarray.

Case No./Age, yr	TNM Classification	Primary Tumor Location
1/43	T3N0M0	Oral tongue
2/56	T3N2bM0	Oral tongue
3/64	T3N2cM0	Oral tongue
4/68	T4N2cM0	Oral tongue
5/50	T3N1Mx	Base of tongue
6/52	T2N2cM0	Base of tongue
7/52	T2N2cM0	Base of tongue
8/59	T2N1M0	Base of tongue
9/60	T1N2aM0	Base of tongue
10/62	T4N2bM0	Base of tongue
11/84	T1N0M0	Base of tongue
12/62	T3N2M0	Supraglottic larynx
13/71	T3N1M0	Supraglottic larynx
14/52	T4aN0Mx	Glottic larynx
15/53	T3N1M0	Glottic larynx
16/59	T4aN2M0	Glottic larynx
17/71	T3N1M0	Glottic larynx
18/74	T2N0M0	Hypopharynx
19/52	T2N0M0	Tonsil
20/59	T1N1M0	Tonsil
21/68	T1N0M0	Tonsil
22/77	T3N2bM0	Tonsil

staining protocol follows. Formalin-fixed, paraffin-embedded samples were first deparaffinized and rehydrated. Antigen retrieval was performed by placing slides in a preheated Dako Target Retrieval buffer followed by cooling in the buffer. Slides were then subject to a protein block and an endogenous peroxidase block. Sections were incubated with the necessary sequence of primary antibodies for 30 minutes at room temperature followed by incubation with streptavidin-peroxidase. Sections were finally incubated in 3,3'-diaminobenzidine and counterstained with hematoxylin. All staining was performed using the appropriate positive and negative controls. In addition, double immunofluorescence staining was performed on a frozen HNSCC tumor specimen to localize FR- $\beta$  and CD68 expression. FR- $\beta$  was stained using biotinylated m909 followed by streptavidin-phycoerythrin. CD68 was stained using FITC conjugated mAb Ki-M7 (Life Technologies, Grand Island, NY). Fluorescence microscopy was performed using the Leica DM5500 microscope (Leica, Wetzlar, Germany).

### TMA Analysis

A head and neck pathologist (J.T.) scored the FR- $\alpha$  and FR- $\beta$  staining of the TMA specimens. Staining intensity was graded as 0+, 1+, 2+, or 3+. The area of specimen staining was given as a percentage of total specimen area in the analyzed section (0%–100%). KB and CHO- $\beta$  cells were used as positive controls for FR- $\alpha$  and FR- $\beta$  staining, respectively. The overall staining pattern of CD68 staining was compared with that of FR- $\alpha$  and FR- $\beta$  but not formally scored. FR staining intensity and area scores were multiplied together for analysis, resulting in a possible combined staining score of 0 to 300. For comparison, primary tumor locations were categorized as either lymphoid (tonsils and base of tongue) or nonlymphoid (all other locations).

## Flow Cytometry

Flow cytometry was performed on tumor and adjacent benign surgical margin tissue samples from two HNSCC patients. Tissues were manually minced, and then 5-mL specimens were digested for 2 hours at 37°C in an enzyme solution containing 0.1% collagenase IV (Sigma-Aldrich, St. Louis, MO) and 0.01% DNase I (Sigma-Aldrich). During digestion, samples were placed in a shaker and also manually mixed every 15 minutes. Single cells were isolated by straining digested tissue through a 40- $\mu$ m cell strainer (BD Biosciences, San Jose, CA) and digestion was halted by washing cells with phosphate-buffered saline (PBS) containing 10% fetal bovine serum (FBS). Erythrocytes were depleted by incubation in red cell lysis buffer (Sigma-Aldrich) for 5 minutes at room temperature. Cells were washed with PBS and suspended in PBS containing 1% FBS.

For FR- $\beta$  detection, single cell suspensions were first incubated with biotinylated m909<sup>19</sup> or biotinylated IgG1 isotype control (Biocare Medical) at a 1:100 dilution for 1 hour at 4°C. Samples were then incubated with streptavidin-phycoerythrin at a 1:200 dilution for another hour. For analysis of CD45 or CD206 coexpression, cells were then incubated in allophycocyanin conjugated mAb HI30 (Life Technologies) or allophycocyanin conjugated mAb 15-2 (Biolegend, San Diego, CA) at a 1:100 dilution for 1 hour. For analysis of TGF- $\beta$  coexpression, cells were first incubated in BD Cytofix/Cytoperm fixation and permeabilization buffer (BD Biosciences) for 20 minutes. Cells were then washed in the BD Perm/Wash solution and incubated with allophycocyanin conjugated mAb TW4-2F8 (Biolegend) at a 1:100 dilution for 1 hour. Flow cytometry was performed on a BD LSRFortessa flow cytometer with FACSDiva software (BD Biosciences), and FlowJo (Tree Star, Ashland, OR) was used for analyzing the data. For data analysis, the fluorescence gate for antibody fluorescence was set so that <1% of the cells appeared to be positive when examined with a nonspecific antibody isotype control.

## Orthotopic Xenograft Model

All animal studies were carried out with the approval by the University of Texas Southwestern Institutional Animal Care and Use Committee. HN5 and FaDu human HNSCC cells were cultured in Dulbecco modified Eagle medium containing 5% FBS, L-glutamine, penicillin, and streptomycin. Cells were incubated at 37°C in 5% CO<sub>2</sub>. Female athymic nude mice (Charles River Laboratories, Wilmington, MA) received an injection of  $5 \times 10^6$  HN5 cells suspended in 100  $\mu$ L of PBS into the suprahyoid muscles. Similarly, severe combined immunodeficiency disorder mice (Taconic, Hudson, NY) received an injection of  $5 \times 10^6$  FaDu or HN5 cells into the same location. Mice were sacrificed for imaging after 2 to 3 weeks of tumor growth. Tumor xenografts grew vigorously and were found to be infiltrating into neck muscles and the base of the tongue.

## Fluorescence Imaging

Two hours before in vivo imaging, mice received tail vein injections of 0.8 mg/kg folate-FITC (produced as EC17; Endocyte Inc., West Lafayette, IN). In vivo and ex vivo images were taken using the Maestro small animal imaging system (CRi, Woburn, MA). Folate-FITC has an excitation wavelength of 495 nm and an emission wavelength of 520 nm. Before in vivo imaging, mice were anesthetized, and skin overlying the lower face, neck, and upper chest was removed. Still images of the mice were taken under white light and fluorescent light. The folate-FITC signal strength in tumor xenograft tissues was calculated using the Maestro imaging system software. The area of visible

TABLE II.  
Immunohistochemistry Analysis of Folate Receptor Expression.

Stain	Characteristic	No.	Mean Staining Score	P Value	
FR- $\alpha$	Tumor	22	0	.281	
	Tumor-free margin	22	1		
FR- $\beta$	Tumor	22	24	.379	
	Primary tumor location				
		Lymphoid rich	11	32	.055
		Lymphoid poor	11	15	
	Tumor stage				
		I, II, III	11	30	.119
		IV	11	17	
	HPV p16 positivity				
		Yes	7	12	.750
		No or not tested	15	11	
	Smoking history				
		Yes	17	10	.114
		No	5	16	
	2-year survival				
		Yes	18	13	.094
		No	4	7	
Tumor-free margin					
	22	19			
Primary tumor location					
	Lymphoid rich	11	11	.015	
	Lymphoid poor	11	28		

Staining score was calculated as the product of a specimen's staining area (0%–100%) and staining intensity (0–3). Lymphoid rich indicates base of tongue and tonsils. Lymphoid poor indicates oral tongue, supra-glottic larynx, glottic larynx, and hypopharynx.

FR = folate receptor; HPV = human papillomavirus.

fluorescent signal as a percentage of total xenograft tumor area was calculated from still images using ImageJ (National Institutes of Health, Bethesda, MD). Mice were then sacrificed, and the entire tumor along with adjacent benign tissues was resected for gross ex vivo imaging followed by frozen sectioning. Before tissue fixation, fluorescent images of the tumors of probe-injected mice were captured using the Leica DM5500 microscope (Leica). Finally, sections were formalin fixed and stained with hematoxylin and eosin (H&E) for comparison with fluorescent images.

## Statistical Analysis

Statistical analysis was performed using JMP 10 (SAS Institute Inc., Cary, NC). Statistical comparisons of paired tumor versus margin staining analysis were made using the Wilcoxon signed rank test. Other unpaired comparisons were made using the Mann-Whitney *U* test. All tests were two-sided. A *P* < .05 was considered statistically significant.

## RESULTS

FR- $\alpha$  staining with mAb 343 was minimal or completely absent in all 22 tumor specimens examined (Table II). Similarly, the benign surgical margins only exhibited FR- $\alpha$  staining in salivary glandular tissue, which has been previously reported to express FR- $\alpha$  (Fig. 1).<sup>11</sup> This result was confirmed by repeated



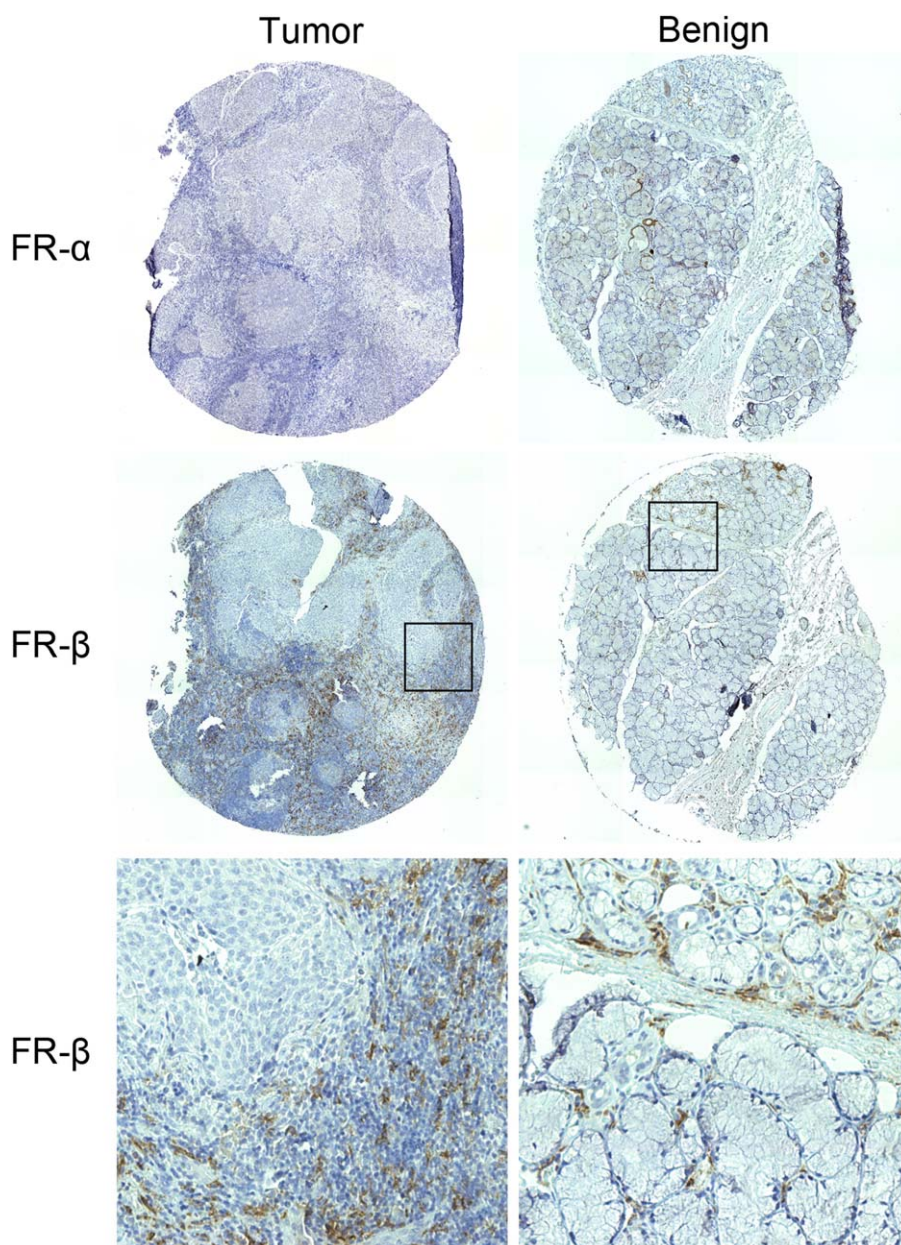


Fig. 1. Representative tumor and matched benign tissue microarray (TMA) specimens from the tonsils stained for folate receptor (FR)- $\alpha$  and FR- $\beta$ . FR- $\alpha$  staining was absent or minimal in tumor and benign specimens. In contrast, FR- $\beta$  staining was seen in most TMA specimens. The FR- $\beta$  staining of the specimens shown was scored as 3+, 15% (intensity, area of specimen) for the tumor and 3+, 3% for the benign tissue. The bottom row represent higher magnification (20 $\times$ ) views of the corresponding boxed areas. Results from other TMA specimens are summarized in Table II. [Color figure can be viewed in the online issue, which is available at [www.laryngoscope.com](http://www.laryngoscope.com).]

staining with a different antibody, mAb 26B3, against FR- $\alpha$ . No FR staining was observed in normal nonglandular epithelial, vascular, adipose, or muscle tissue. In

contrast, all tumor specimens were moderately to strongly positive for FR- $\beta$  staining (Table II and Fig. 1). The adjacent benign surgical margins also exhibited

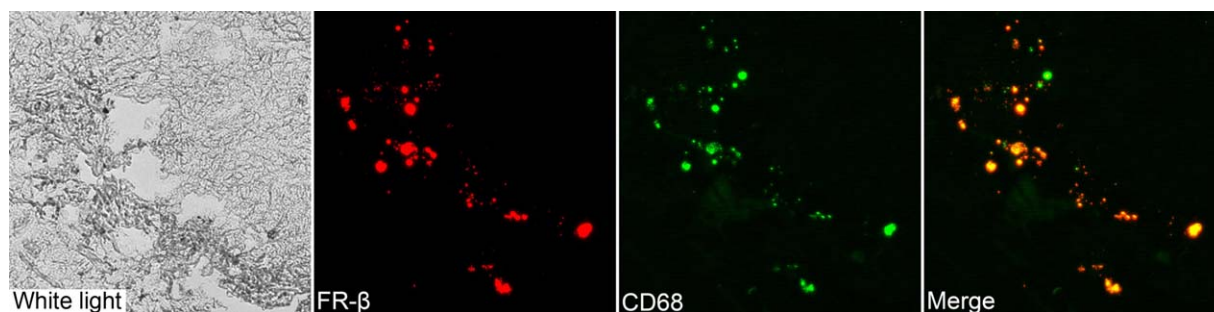


Fig. 2. Dual immunofluorescence of tumor tissue for folate receptor- $\beta$  (red) and the macrophage marker CD68 (green) demonstrates strong signal colocalization (20 $\times$ ). [Color figure can be viewed in the online issue, which is available at [www.laryngoscope.com](http://www.laryngoscope.com).]

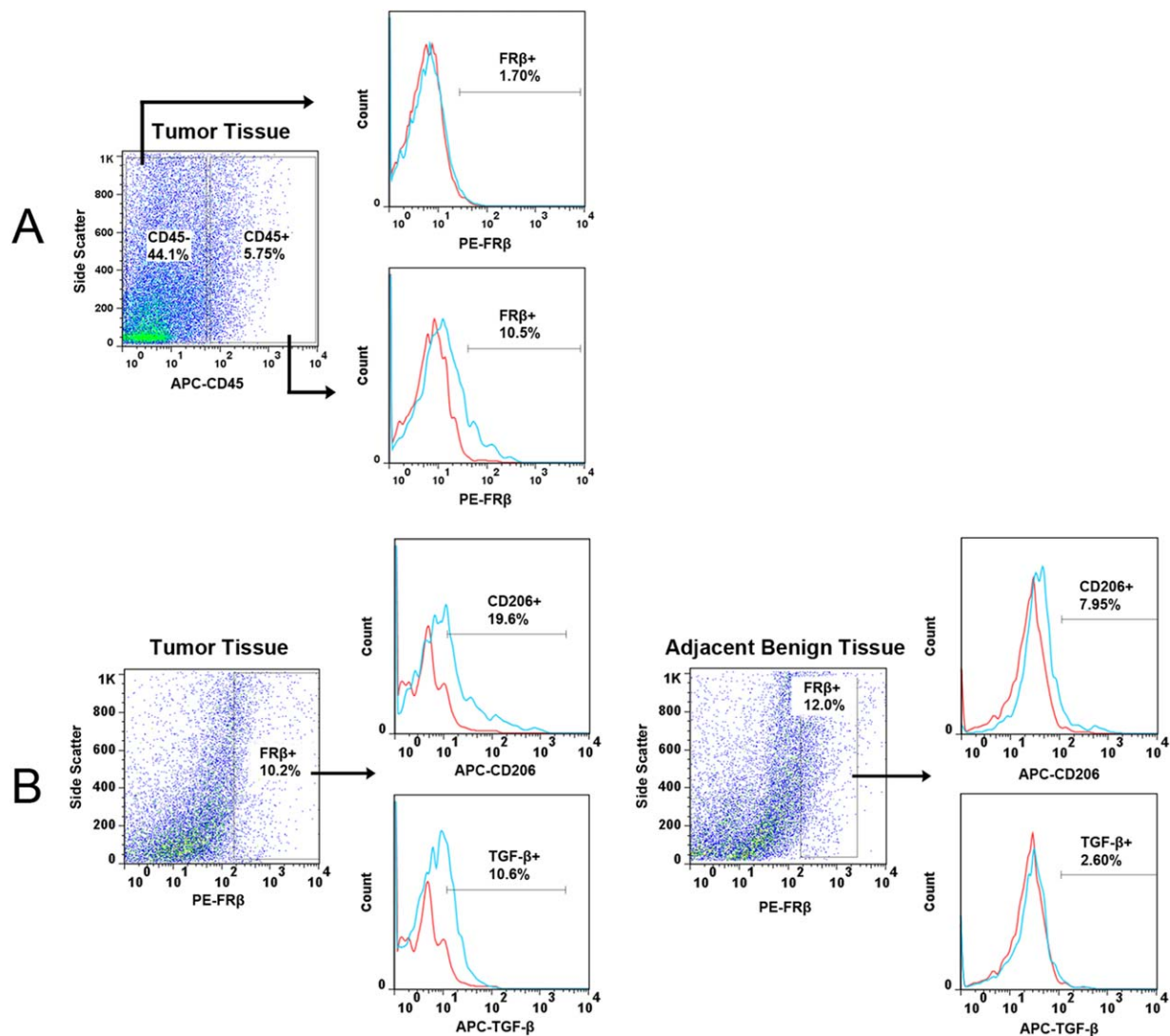


Fig. 3. Flow cytometric analysis of folate receptor (FR)- $\beta^+$  cells from human tissues. Red and blue lines on histograms represent cells stained with matched isotype immunoglobulin G controls and cells stained with corresponding monoclonal antibodies respectively. (A) Histogram shows the percentage of FR- $\beta^+$  cells in CD45 $^+$  and CD45 $^-$  cell populations. FR- $\beta^+$  cells are only found in the CD45 $^+$  hematopoietic cell population. (B) Histograms show the percentage of CD206 $^+$  and TGF- $\beta^+$  cells in the FR- $\beta^+$  cell population from the tumor and the adjacent benign surgical margin. Compared to the surgical margin, FR- $\beta^+$  cells from the tumor were found to express more of both M2 markers. TGF- $\beta$  = transforming growth factor  $\beta$ , APC = Allophycocyanin, PE = Phycoerythrin. [Color figure can be viewed in the online issue, which is available at [www.laryngoscope.com](http://www.laryngoscope.com).]

moderate to strong FR- $\beta$  staining. FR- $\beta$  expression in tumor specimens and the adjacent benign surgical margins occurred solely in infiltrating inflammatory cells (Fig. 1). The epithelial cancer cells showed no signs of FR- $\beta$  staining.

Immunohistochemistry and flow cytometry were used to further characterize the FR- $\beta$ -expressing cells found in HNSCC. Double immunofluorescence labeling of FR- $\beta$  and the macrophage marker, CD68, showed strong colocalization between the two receptors (Fig. 2). Flow cytometric analysis of tumor and benign margin tissues samples demonstrated that cells positive for FR- $\beta$  were indeed hematopoietic cells as indicated by CD45 expression (Fig. 3). TGF- $\beta$  and mannose receptor (CD206) were used in flow cytometry as markers for alternatively activated (M2) macrophages.<sup>20</sup> FR- $\beta$ -

expressing cells from tumor tissue showed increased expression of both of these M2-related markers compared to FR- $\beta$ -expressing cells found in the benign tumor margin (Fig. 3).

To examine whether the local anatomy of the excised tissue affected FR staining, the specimens were divided into two categories based on the location of the primary tumor—lymphoid (base of tongue and tonsils) or nonlymphoid (oral tongue, larynx and hypopharynx). Differences in the FR- $\beta$  staining of tumor specimens between these categories did not reach significance (Table II). On the other hand, benign margins from the base of tongue and tonsils had less FR- $\beta$  staining than margins taken from nonlymphoid tissues, suggesting that the FR- $\beta^+$  leukocytes in the margins are not a consequence of normal lymphoid tissue. Because nearly all



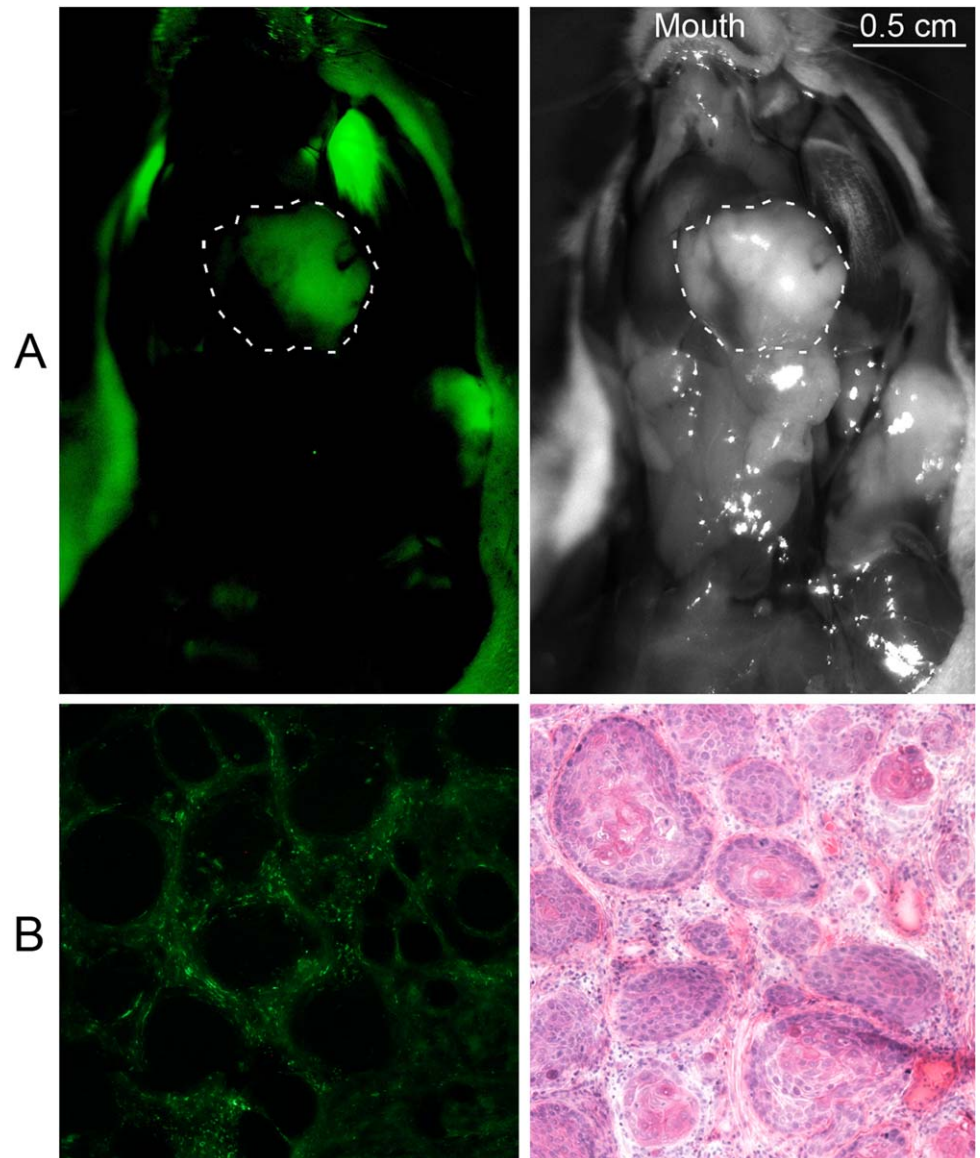


Fig. 4. Folate conjugated fluorescein isothiocyanate (folate-FITC) targeting to head and neck tumor xenograft. (A) Fluorescent and white light in vivo images of ventral mouse head and neck with tumor outlined after folate-FITC injection. Fur in the background exhibits autofluorescence unrelated to folate-FITC uptake. The signal of the tumor shown was 63 counts/pixel. The combined average signal of the nearby normal salivary glands, lymph nodes, and muscles was 4.5 counts/pixel, yielding a tumor-to-background signal ratio of 14. (B) Fluorescent microscopy and hematoxylin and eosin staining of mouse tumor section (10 $\times$ ). Folate-FITC uptake is seen in the tumor stroma but not within tumor cells. [Color figure can be viewed in the online issue, which is available at [www.laryngoscope.com](http://www.laryngoscope.com).]

the tumor specimens were from patients with already advanced-stage cancer, no relationship was found between FR- $\beta$  expression and the pathological stage of the tumors (Table II). There was no significant relationship between FR- $\beta$  staining and human papillomavirus status, smoking history, or 2-year absolute survival (Table II).

After demonstrating the presence of folate-receptor-expressing inflammatory cells in the HNSCC tumor microenvironment, we examined folate-FITC targeting to head and neck cancer in vivo with orthotopic xenograft models. In both HN5 and FaDu cell line implanted mice, folate-FITC fluoresced strongly in regions of the tumor (Fig. 4). Analysis of still images revealed that 6% to 39% (mean, 25%;  $n = 6$ ) of the tumor area displayed visible folate-FITC fluorescence. Benign tissues including the salivary glands, lymph nodes, oral mucosa, and muscle did not exhibit visible fluorescent signal. Compared with FR- $\alpha$ -expressing salivary glands, the tumor

had a 3- to 30-fold higher total signal intensity (mean, 12-fold increase;  $n = 6$ ). Under the excitation wavelength that we used, normal skin and fur of the mice exhibited autofluorescence unrelated to folate-FITC uptake.

To determine whether the fluorescent tumor regions seen in the xenograft models correlated with the FR- $\beta$ -expressing regions seen in the TMA, tumors sections were examined with fluorescent microscopy and H&E staining. Consistent with the FR- $\beta$  staining pattern seen in the TMA, folate-FITC fluorescence was localized to the inflammatory stroma of the tumor and absent in the tumor cells (Fig. 4).

## DISCUSSION

FR- $\beta$ -expressing macrophages have been reported in the synovium of rheumatoid arthritis patients and in malignant tumors.<sup>21-23</sup> The effect of inflammatory cells on tumor progression has long been appreciated.<sup>24</sup>

By promoting angiogenesis, lymphangiogenesis, tissue remodeling, immunosuppression, and tumor invasion through the production of TGF- $\beta$  and other factors characteristic of the M2 macrophage lineage, tumor-associated macrophages (TAM), in particular, are correlated with poor prognosis in a variety of malignancies.<sup>25</sup> FR- $\beta^+$  TAM have been extracted from melanoma and breast adenocarcinoma and characterized as interleukin (IL)-10-expressing anti-inflammatory M2 macrophages.<sup>22</sup> In pancreatic cancer, FR- $\beta^+$  macrophages coexpress vascular endothelial growth factor, and higher numbers of these cells are linked to an increased incidence of metastasis and a poorer prognosis.<sup>23</sup> These studies suggest that TAM with the FR- $\beta$  phenotype may promote tumor progression at least partially through immunosuppressive and angiogenic influences.<sup>22,23</sup> Our observations of CD68 colocalization on immunohistochemistry and increased M2 marker signal on flow cytometry, suggest the FR- $\beta^+$  inflammatory cells found in HNSCC tumors most likely represent FR- $\beta^+$  TAM as well. However, the exact physiologic actions of FR- $\beta^+$  TAM and of the folate receptor itself are uncertain. The fact that FR- $\beta^+$  macrophages appear to exert both proinflammatory and anti-inflammatory effects in rheumatoid arthritis and cancer, respectively, indicates that the immunology of these cells is highly complicated.<sup>21,22</sup> The significance of FR- $\beta$ -expressing macrophages in HNSCC remains unknown.

Saba et al. reported that folate receptor is expressed in some HNSCC tumors, and that higher expression is linked with poorer prognosis.<sup>17</sup> We did not observe folate receptor expression directly in the head and neck cancer cells. This discrepancy may be due to the polyclonal, non-isotype-specific antibody used by Saba et al. to detect FR, which exhibits binding to other FR isotypes on benign cells in addition to nonspecific binding associated with its polyclonal nature. Our study used two different highly specific monoclonal antibodies against FR- $\alpha$  that have both previously been employed in immunohistochemistry to detect FR on cancer cells.<sup>18,26</sup> Additionally, their observation that FR expression negatively correlates with disease-free survival in HNSCC may be due to the detection of the FR- $\beta^+$  TAM that we describe here. Furthermore, because we did not find FR expression on cancer cells, folate-linked anticancer drugs, an area of active research, would not be able to effectively target cancer cells in HNSCC, but instead would target associated TAM.

Optical imaging of HNSCC under fluorescent light is feasible through the targeting of folate-FITC to cells in the inflammatory tumor microenvironment. Normal tissue, including lymphocytes within lymph nodes, do not exhibit folate-FITC uptake, highlighting the specific upregulation of FR- $\beta^+$  in TAM and allowing specific optical visualization of the tumor. However, inflammatory cell infiltration into the tumors is variable, leading to heterogeneous fluorescence. Although this effect does not impede the macroscopic detection of tumor nodules, it can limit the ability of folate-FITC to aid in the intraoperative determination of HNSCC tumor margins. Folate conjugated therapeutic targeting of TAM, how-

ever, may be a viable avenue for drug delivery. It is also unknown whether a folate probe can facilitate the detection of lymph node metastasis or high-risk sentinel lymph nodes. We only examined primary tumors for FR- $\beta$  expression. TAM are known to promote lymphangiogenesis in the primary tumor through vascular endothelial growth factor C and may even invade regional lymph nodes ahead of the tumor to prepare them for metastasis.<sup>27,28</sup> However, this phenotype has not been investigated in association with FR- $\beta$  expression or in head and neck cancer. Detailed study of FR- $\beta$  expression and TAM in regional lymph nodes in HNSCC may be important.

In addition to a molecular probe's tumor-targeting ability, the choice of conjugated fluorophore also has a significant impact on tumor detection and image quality. In this study, we employed folate conjugated to FITC dye in particular due to the probe's documented use in human trials, extensive characterization in other animal models, and ready availability.<sup>9</sup> However, fluorophores emitting in the near-infrared (NIR) spectrum offer the advantages of having minimal tissue autofluorescence and better tissue penetration compared to fluorophores with shorter wavelength emissions such as FITC. For image-guided surgery, NIR may be ideal. NIR dye conjugated tumor targeting antibody probes have begun clinical trials for HNSCC and rectal cancer detection.<sup>29,30</sup> Recently, folate has also been conjugated to NIR dyes.<sup>31</sup> Given the autofluorescence observed in our mice while imaging for folate-FITC, we suspect that an NIR dye conjugated folate probe would result in improved tumor imaging quality.

## CONCLUSION

We demonstrate that HNSCC tumors contain a significant population of FR- $\beta$ -expressing stromal cells. Our characterization of these FR- $\beta^+$  cells suggests that they are tumor-associated macrophages. In contrast to many other carcinomas, the HNSCC tumor cells in our TMA did not express FR- $\alpha$ . Despite the lack of tumor cell FR expression, the folate-FITC fluorescent probe was able to specifically label tumor xenografts in mice by targeting the infiltrating FR- $\beta^+$  inflammatory cells. The folate receptor on the described macrophages may represent a convenient target for the delivery of folate conjugated imaging agents and drugs into the HNSCC tumor microenvironment.

## BIBLIOGRAPHY

1. American Cancer Society. *Cancer Facts & Figures* 2012. Atlanta, GA: American Cancer Society; 2012.
2. Bernier J, Domenge C, Ozsahin M, et al. Postoperative irradiation with or without concomitant chemotherapy for locally advanced head and neck cancer. *N Engl J Med* 2004;350:1945-1952.
3. Hadjipanayis CG, Jiang H, Roberts DW, Yang L. Current and future clinical applications for optical imaging of cancer: from intraoperative surgical guidance to cancer screening. *Semin Oncol* 2011;38:109-118.
4. Rosenthal EL, Kulbersh BD, Duncan RD, et al. In vivo detection of head and neck cancer orthotopic xenografts by immunofluorescence. *Laryngoscope* 2006;116:1636-1641.
5. Heath CH, Deep NL, Sweeny L, Zinn KR, Rosenthal EL. Use of panitumumab-IRDye800 to image microscopic head and neck cancer in an orthotopic surgical model. *Ann Surg Oncol* 2012;19:3879-3887.

6. Nguyen QT, Olson ES, Aguilera TA, et al. Surgery with molecular fluorescence imaging using activatable cell-penetrating peptides decreases residual cancer and improves survival. *Proc Natl Acad Sci USA* 2009; 107:4317–4322.
7. Looser KG, Shah JP, Strong EW. The significance of “positive” margins in surgically resected epidermoid carcinomas. *Head Neck* 1978;1:107–111.
8. McMahon J, O'Brien CJ, Pathak I, et al. Influence of condition of surgical margins on local recurrence and disease-specific survival in oral and oropharyngeal cancer. *Br J Oral Maxillofac Surg* 2003;41:224–231.
9. van Dam GM, Themelis G, Crane LMA, et al. Intraoperative tumor-specific fluorescence imaging in ovarian cancer by folate receptor- $\alpha$  targeting: first in-human results. *Nat Med* 2011;17:1315–1319.
10. Keereweer S, Mieog JD, Mol IM, et al. Detection of oral squamous cell carcinoma and cervical lymph node metastasis using activatable near-infrared fluorescence agents. *Arch Otolaryngol Head Neck Surg* 2011; 137:609–615.
11. Salazar MD, Ratnam M. The folate receptor: what does it promise in tissue-targeted therapeutics? *Cancer Metastasis Rev* 2007;26:141–152.
12. Parker N, Turk M, Westrick E, Lewis JD, Low PS, Leamon CP. Folate receptor expression in carcinomas and normal tissues determined by a quantitative radio-ligand binding assay. *Anal Biochem* 2005;338: 284–293.
13. Kalli KR, Oberg AL, Keeney GL, et al. Folate receptor alpha as a tumor target in epithelial ovarian cancer. *Gynecol Oncol* 2008;108:619–626.
14. Cagle PT, Zhai Q, Murphy L, Low PS. Folate Receptor in adenocarcinoma and squamous cell carcinoma of the lung: potential target for folate-linked therapeutic agents. *Arch Pathol Lab Med* 2013;137:241–244.
15. Ross JF, Wang H, Behm FG, et al. Folate receptor type  $\beta$  is a neutrophilic lineage marker and is differentially expressed in myeloid leukemia. *Cancer* 1999;85:348–357.
16. Ross JF, Chaudhuri PK, Ratnam M. Differential regulation of folate receptor isoforms in normal and malignant tissues in vivo and in established cell lines. *Cancer* 1994;73:2432–2443.
17. Saba NF, Wang X, Muller S, et al. Examining expression of folate receptor in squamous cell carcinoma of the head and neck as a target for a novel nanotherapeutic drug. *Head Neck* 2009;31:475–481.
18. O'Shannessy DJ, Yu G, Smale R, et al. Folate receptor alpha expression in lung cancer: diagnostic and prognostic significance. *Oncotarget* 2012;3: 414–425.
19. Feng Y, Shen J, Streaker ED, et al. A folate receptor beta-specific human monoclonal antibody recognizes activated macrophage of rheumatoid patients and mediates antibody-dependent cell-mediated cytotoxicity. *Arthritis Res Ther* 2011;13:R59.
20. Heusinkveld M, van der Burg SH. Identification and manipulation of tumor associated macrophages in human cancers. *J Transl Med* 2011;9:216.
21. Wei X, Hilgenbrink AR, Matteson EL, Lockwood MB, Cheng J, Low PS. A functional folate receptor is induced during macrophage activation and can be used to target drugs to activated macrophages. *Blood* 2009;113: 438–446.
22. Puig-Kroger A, Sierra-Filardi E, Dominguez-Soto A, et al. Folate receptor  $\beta$  is expressed by tumor-associated macrophages and constitutes a marker for M2 anti-inflammatory/regulatory macrophages. *Cancer Res* 2009;69:9395–9403.
23. Kurahara H, Takao S, Kuwahata T, et al. Clinical significance of folate receptor  $\beta$ -expressing tumor-associated macrophages in pancreatic cancer. *Ann Surg Oncol* 2012;19:2264–2271.
24. Coussens LM, Werb Z. Inflammation and cancer. *Nature* 2002;420:860–867.
25. Allavena P, Sica A, Garlanda C, Mantovani A. The yin-yang of tumor associated macrophages in neoplastic progression and immune surveillance. *Immunol Rev* 2008;222:155–161.
26. Jones MB, Neuper C, Clayton A, et al. Rationale for folate receptor alpha targeted therapy in “high risk” endometrial carcinomas. *Int J Cancer* 2008;123:1699–1703.
27. Schoppmann SF, Fenzl A, Nagy K, et al. VEGF-C expressing tumor-associated macrophages in lymph node positive breast cancer: impact on lymphangiogenesis and survival. *Surgery* 2003;139:839–846.
28. Kurahara H, Takao S, Maemura K, et al. M2-polarized tumor-associated macrophage infiltration of regional lymph nodes is associated with nodal lymphangiogenesis and occult nodal involvement in pN0 pancreatic cancer. *Pancreas* 2013;42:155–159.
29. University of Alabama at Birmingham. Cetuximab IRDye800 study as an optical imaging agent to detect cancer during surgical procedures. ClinicalTrials website. Available at: <http://clinicaltrials.gov/ct2/show/NCT01987375>. Updated November 12, 2013. Accessed December 29, 2013.
30. University Medical Centre Groningen, Dutch Cancer Society. Visualization of rectal cancer during endoscopy, using a fluorescent tracer (RAPIDOTRACT). ClinicalTrials website. Available at: <http://clinicaltrials.gov/show/NCT01972373>. Updated October 24, 2013. Accessed December 29, 2013.
31. Kelderhouse LE, Chelvam V, Wayua C, et al. Development of tumor-targeted near infrared probes for fluorescence guided surgery. *Bioconjug Chem*. 2013;24:1075–1080.